4-2014

High-throughput fluorescence-activated cell sorting for lipid hyperaccumulating Chlamydomonas reinhardtii mutants

Bo Xie
Iowa State University

Dan Stessman
Iowa State University

Jason H. Hart
Iowa State University

Haili Dong
Iowa State University

Yingjun Wang
Iowa State University

High-throughput fluorescence-activated cell sorting for lipid hyperaccumulating Chlamydomonas reinhardtii mutants

Abstract

The genetically tractable microalga Chlamydomonas reinhardtii has many advantages as a model for renewable bioproducts and/or biofuels production. However, one limitation of C. reinhardtii is its relatively low-lipid content compared with some other algal species. To overcome this limitation, we combined ethane methyl sulfonate mutagenesis with fluorescence-activated cell sorting (FACS) of cells stained with the lipophilic stain Nile Red to isolate lipid hyperaccumulating mutants of C. reinhardtii. By manipulating the FACS gates, we sorted mutagenized cells with extremely high Nile Red fluorescence signals that were rarely detected in nonmutagenized populations. This strategy successfully isolated several putative lipid hyperaccumulating mutants exhibiting 23% to 58% (dry weight basis) higher fatty acid contents than their progenitor strains. Significantly, for most mutants, nitrogen starvation was not required to attain high-lipid content nor was there a requirement for a deficiency in starch accumulation. Microscopy of Nile Red stained cells revealed that some mutants exhibit an increase in the number of lipid bodies, which correlated with TLC analysis of triacyglycerol content. Increased lipid content could also arise through increased biomass production. Collectively, our findings highlight the ability to enhance intracellular lipid accumulation in algae using random mutagenesis in conjunction with a robust FACS and lipid yield verification regime. Our lipid hyperaccumulating mutants could serve as a genetic resource for stacking additional desirable traits to further increase lipid production and for identifying genes contributing to lipid hyperaccumulation, without lengthy lipid-induction periods.

Keywords

Chlamydomonas reinhardtii, lipid hyperaccumulation, Nile Red, mutagenesis, fluorescence-activated cell sorting

Disciplines

Genetics and Genomics | Plant Breeding and Genetics

Comments

This article is published as Xie, Bo, Dan Stessman, Jason H. Hart, Haili Dong, Yingjun Wang, David A. Wright, Basil J. Nikolau, Martin H. Spalding, and Larry J. Halverson. "High-throughput fluorescence-activated cell sorting for lipid hyperaccumulating Chlamydomonas reinhardtii mutants." Plant biotechnology journal 12, no. 7 (2014): 872-882. 10.1111/pbi.12190. Posted with permission.

Authors

Bo Xie, Dan Stessman, Jason H. Hart, Haili Dong, Yingjun Wang, David A. Wright, Basil J. Nikolau, Martin H. Spalding, and Larry J. Halverson

Plant Biotechnology Journal

Plant Biotechnology Journal (2014) **12**, pp. 872–882 doi: 10.1111/pbi.12190

High-throughput fluorescence-activated cell sorting for lipid hyperaccumulating *Chlamydomonas reinhardtii* mutants

Bo Xie[1,†], Dan Stessman[2], Jason H. Hart[3], Haili Dong[2], Yingjun Wang[2], David A. Wright[2], Basil J. Nikolau[3,4], Martin H. Spalding[2,4] and Larry J. Halverson[1,4,*]

[1]*Department of Plant Pathology & Microbiology, Iowa State University, Ames, IA, USA*
[2]*Genetics, Development & Cell Biology, Iowa State University, Ames, IA, USA*
[3]*Department of Biochemistry, Biophysics & Molecular Biology, and Center for Metabolic Biology, Iowa State University, Ames, IA, USA*
[4]*Plant Sciences Institute, Iowa State University, Ames, IA, USA*

Received 17 October 2013;
revised 3 January 2014;
accepted 26 February 2014.
**Correspondence* (Tel +1 515 294 0495;
fax +1 515 294 6019;
email larryh@iastate.edu)
†Present address: School of Life Sciences, Central China Normal University, Wuhan, 430079, China.

Keywords: *Chlamydomonas reinhardtii*, lipid hyperaccumulation, Nile Red, mutagenesis, fluorescence-activated cell sorting.

Summary

The genetically tractable microalga *Chlamydomonas reinhardtii* has many advantages as a model for renewable bioproducts and/or biofuels production. However, one limitation of *C. reinhardtii* is its relatively low-lipid content compared with some other algal species. To overcome this limitation, we combined ethane methyl sulfonate mutagenesis with fluorescence-activated cell sorting (FACS) of cells stained with the lipophilic stain Nile Red to isolate lipid hyperaccumulating mutants of *C. reinhardtii*. By manipulating the FACS gates, we sorted mutagenized cells with extremely high Nile Red fluorescence signals that were rarely detected in nonmutagenized populations. This strategy successfully isolated several putative lipid hyperaccumulating mutants exhibiting 23% to 58% (dry weight basis) higher fatty acid contents than their progenitor strains. Significantly, for most mutants, nitrogen starvation was not required to attain high-lipid content nor was there a requirement for a deficiency in starch accumulation. Microscopy of Nile Red stained cells revealed that some mutants exhibit an increase in the number of lipid bodies, which correlated with TLC analysis of triacyglycerol content. Increased lipid content could also arise through increased biomass production. Collectively, our findings highlight the ability to enhance intracellular lipid accumulation in algae using random mutagenesis in conjunction with a robust FACS and lipid yield verification regime. Our lipid hyperaccumulating mutants could serve as a genetic resource for stacking additional desirable traits to further increase lipid production and for identifying genes contributing to lipid hyperaccumulation, without lengthy lipid-induction periods.

Introduction

Interest in a variety of renewable biofuels has increased recently, with particular focus on photosynthetic microalgae for harvesting lipids that can be used for liquid fuels (Beer *et al.*, 2009; Hu *et al.*, 2008; Merchant *et al.*, 2012; Radakovits *et al.*, 2010). A widely adopted approach is to identify oleaginous algal species and to extract and process their oils. Although not known to be a high-lipid producing alga, *Chlamydomonas reinhardtii* has received increased attention as a model for biofuel production because of its highly developed biochemical, molecular and genetic tools (Harris, 2009; Merchant *et al.*, 2007; Radakovits *et al.*, 2010) and recent studies demonstrating that N-deficient cells can accumulate triacylglycerol (TAG) in considerable amounts, particularly in strains deficient in starch accumulation (James *et al.*, 2011; Li *et al.*, 2010; Siaut *et al.*, 2011; Work *et al.*, 2010). Although presently, *C. reinhardtii* yields are unsuitable for a production strain, understanding how to genetically manipulate lipid content and biomass yields will guide improvements of this and other algal species (Radakovits *et al.*, 2010).

Triacylglycerol is stored in subcellular structures often referred to as lipid droplets or lipid bodies (Goodson *et al.*, 2011). Many wild-type *C. reinhardtii* strains produce a small number of lipid bodies in the cytosol during normal growth but their number and size can increase substantially when cultures are deprived of nitrogen or other nutrients (Goodson *et al.*, 2011; Wang *et al.*, 2009). Upon N-starvation, starch-forming cells initially partition resources to starch biosynthesis, but after prolonged N-deprivation, lipid bodies form in the cytoplasm that are intimately associated with both the outer membrane of the chloroplast and the endoplasmic reticulum (Goodson *et al.*, 2011). However, N-deprived starchless cells immediately divert excess carbon to form lipid bodies in the cytosol and chloroplast. Lipid body production is boosted by excess carbon, frequently through an acetate boost (Fan *et al.*, 2012; Goodson *et al.*, 2011), but also photoautotrophically in atmospheres enriched in CO_2 (Li *et al.*, 2010; Merchant *et al.*, 2012). The ability to visualize lipid bodies has been facilitated by use of the lipophilic dye Nile Red (9-diethylamino-5H-benzo[α]phenoxazine-5-one) that fluoresces a specific yellow wavelength when interacting with neutral lipids (Cooksey *et al.*, 1987; Greenspan and Fowler, 1985; Hyka *et al.*, 2013). Consequently, there has been much interest in using Nile Red as an alternative to lipid content determinations for measuring neutral lipid contents of a variety of algal species by fluorometry or flow cytometry, and for isolating strains that accumulate more neutral lipids by fluorescence-activated cell

sorting (FACS) (Chen *et al.*, 2009; Cooksey *et al.*, 1987; Doan and Obbard, 2012; Li *et al.*, 2010; Montero *et al.*, 2011).

There are several approaches for genetic engineering *C. reinhardtii* to modify lipid production. For example, directed engineering of known metabolic networks to alter neutral lipid accumulation, such as by overexpressing diacylglycerol acyltransferases (DGAT), the enzyme catalyzing the final step in TAG synthesis from diacylglycerol and acyl-CoA (La Russa *et al.*, 2012) or RNA interference to modulate lipid droplet size (Moellering and Benning, 2010). An alternative is a genetic approach employing mutagenesis and screening of mutagenized populations to identify mutants with desirable traits without *a priori* knowledge of components that either relieve constraints on neutral lipid accumulation or block synthesis of alternative, nonessential products. Such mutants can then be used to elucidate molecular processes influencing neutral lipid accumulation or other attributes contributing to high productivity as well as serving as recipient of transgenes for metabolic engineering.

This study describes a high-throughput procedure for identifying mutant *C. reinhardtii* strains with inherently different neutral lipid accumulation patterns. Our strategy was to use FACS of Nile Red stained mutagenized populations to identify putative mutants with Nile Red fluorescence intensities substantially greater than the vast majority of the progenitor line. Once isolated, these putative mutants were characterized in photobioreactors (PBRs) to validate lipid accumulation and fatty acid profile patterns were determined under various cultivation conditions. We also compared Nile Red staining with TAG accumulation determined by chromatographic techniques. Our result demonstrates the feasibility of this procedure, providing a suite of mutants indicating that manipulation of nitrogen availability is not required to attain high-lipid content nor is there a requirement for a deficiency in starch accumulation to achieve higher lipid content comparable with low-starch mutants. Increased lipid accumulation can also arise through increased biomass production. These mutants provide a resource for identifying genes involved in lipid accumulation or other physiological processes and for metabolic engineering for high-value biorenewable products such as fuel or chemicals.

Results

We report the results of two separate experiments to isolate lipid hyperaccumulating mutants of *C. reinhardtii.* These experiments were conducted with two *C. reinhardtii* strains with inherently different basal lipid levels. Our strategy was comprised of the following elements: (i) random mutagenesis with ethane methyl sulfonate (EMS); (ii) nitrogen-deprivation induction of lipid accumulation (Boyle *et al.*, 2012; James *et al.*, 2011; Moellering and Benning, 2010); (iii) Nile Red staining of neutral lipids; (iv) FACS of cells with Nile Red fluorescence intensities substantially greater than the vast majority of the progenitor line; and (v) validation of lipid contents (Figure 1a). We assumed that mutants accumulating high levels of neutral lipids (i.e. TAG) should exhibit Nile Red fluorescence intensities greater than the progenitor strain. Thus, we established FACS sorting gates to identify cells with extremely high Nile Red fluorescence and normal chlorophyll signals (Figure 1b).

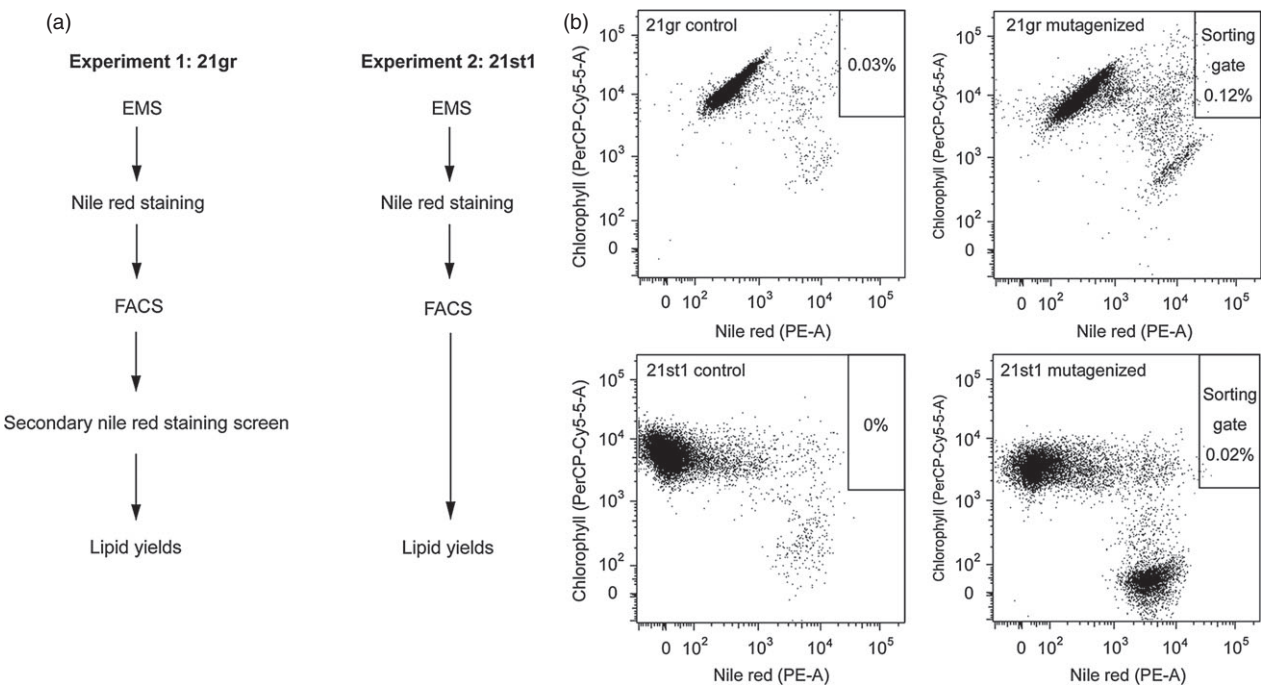

Figure 1 Overview of *Chlamydomonas reinhardtii* lipid hyperaccumulating mutant isolation protocol and fluorescence-activated cell sorting (FACS) of mutagenized cells. (a) Schematic diagrams illustrating the work flow for isolating 21gr (Experiment 1) and 21st1 (Experiment 2) lipid hyperaccumulating mutants. (b) Dot blots of control and mutagenized 21gr and 21st1 populations for establishing sorting gates used for isolating by FACS mutants with Nile Red fluorescence signals greater than the majority of the nonmutagenized progenitor strain. For 21gr, 1.3×10^8 mutagenized cells were examined and 0.12% exhibited Nile Red fluorescence intensities in our sorting gate. For 21st1, 7×10^8 mutagenized cells were examined and 0.02% exhibited Nile Red Fluorescence intensities in our sorting gate.

Screening mutants using FACS

In our first experiment with wild-type strain 21gr, the EMS mutagenesis kill rate was 65%, and following the recovery and nitrogen-deprivation induction period, we subjected 1.3×10^8 cells to FACS. We recovered 5200 putative mutants from the mutagenized population in the sorting gate (Figure 1b), of which 47 of the 2500 colonies examined exhibited a Nile Red bright colony phenotype on media amended with Nile Red, as determined by visual inspection of colonies by epifluorescence microscopy. To be considered a 'Nile Red bright' colony the Nile Red fluorescence had to exceed that of nonmutagenized 21gr colonies (Figure S1). Given that many mutants did not exhibit a Nile Red bright colony phenotype, we chose to screen a subset of non-Nile Red bright colonies to assess the comparative efficacy of high-throughput Nile Red staining of liquid cultures with that of the Nile Red bright colony phenotype.

Mutants were re-suspended in microtitre plates in media with and without nitrogen and incubated for 3 days before determining the Nile Red fluorescence of nitrogen-free relative to nitrogen-amended cultures. Mutants were screened without replication and only rescreened if they exhibited at least 1.5-fold greater Nile Red fluorescence than 21gr. On a cell-density basis, only 33 of 2400 (1.4%) non-Nile Red bright colony mutants whereas 35 of 47 (74%) Nile Red bright colony mutants exhibited Nile Red fluorescence intensities greater than the 21gr strain ($n \geq 3$).

Total lipid content

We selected 33 mutants exhibiting a Nile Red bright colony phenotype and eight non-Nile Red bright colony mutants that exhibited the highest Nile Red fluorescence intensities in liquid culture and analyzed their lipid content. Strains were grown in PBRs, and cells were collected for lipid, biomass and starch analyses 36 h after the onset of stationary phase or following a 36 h nitrogen-deprivation lipid-induction period. In preliminary studies, we determined lipid-induction periods of 0–48 h had little effect on 21gr lipid contents (Table S1), consistent with an earlier report on lipid body production by *C. reinhardtii* (Wang *et al.*, 2009). The relatively short lipid-induction period should facilitate the identification of mutants with rapid lipid accumulation responses. Each mutant was cultivated without replication and rescreened only if lipid content was at least 10% greater than 21gr.

From these analyses, we identified three mutant classes, those with increased lipid content (i) in both stationary phase and an N-deprivation treatments ($n = 9$), (ii) only in stationary phase ($n = 2$), and (iii) only following an N-deprivation treatment ($n = 3$) (Figure 2 and data not shown). Mutants g8, g9, g23, g31 and g35 exhibited a Nile Red bright colony phenotype, whereas g22 and g30 did not (Figure 2). Harvesting cells in stationary phase or following an N-deprivation treatment resulted in 37–55% and 23–36% increase in lipid content relative to 21gr, respectively (Figure 2a). Lipid yields on a per culture volume basis (Figure 2b) were greatly influenced by biomass yields

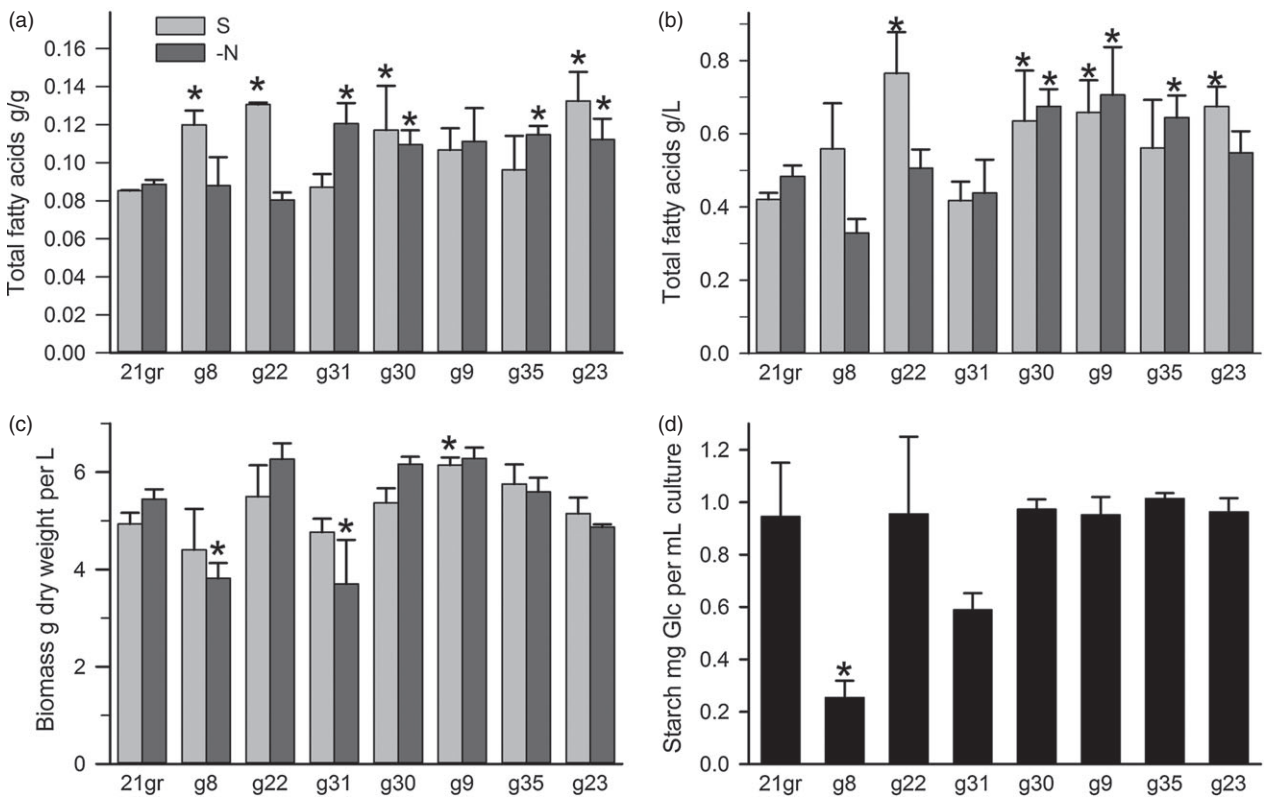

Figure 2 Lipid contents (a) and yields (b), biomass yields (c) and starch contents (d) of 21gr mutants. Data are means ± SE from three independent assays. Biomass values for lipid analyses were obtained 36 h after the onset of stationary phase (S) or following a 36 h lipid-induction treatment in nitrogen-free medium (-N). Separate ANOVAs were performed on each treatment, and asterisks above bars indicate values are statistically different from wild-type 21gr based on a student's *t*-test ($P < 0.05$).

(Figure 2c), most notably the statistically significant greater biomass of mutant g30 in the stationary phase and lower biomass productivity of g8, g31 and g23 in the N-deprivation treatment relative to 21gr. Mutant g22, with slightly elevated biomass (Figure 2b) and high-lipid content (Figure 2a) in stationary phase, yielded 93% more lipids than 21gr. Significantly, many of the mutants could accumulate high levels of lipid without being deficient in starch accumulation (Figure 2d). The growth rates of the mutants were comparable to 21gr (data not shown). Collectively, our data suggest that for most mutants, nitrogen starvation was not required to attain high-lipid content nor was there a requirement for a deficiency in starch accumulation, indicating that increased lipid accumulation occurred in a manner other than re-partitioning carbon reserves from starch and that repression of lipid accumulation by nitrogen availability can be overcome.

TAG accumulation

Neutral lipid can be detected easily by observation of Nile Red stained lipid bodies, and the extent of Nile Red staining per cell can be measured by flow cytometry. As shown visually and quantitatively (Figure 3), several lipid hyperaccumulating mutants contained more lipid bodies than 21gr in stationary phase. Furthermore, Nile Red fluorescence is positively correlated with TAG accumulation determined by TLC (Figure 4). Importantly, Nile Red fluorescence intensities measured by flow cytometry parallel the total lipid content patterns and TAG accumulation by these mutants (Compare Figures 2–4). Flow cytometry indicates a uniform increase in Nile Red staining in the mutant population compared with 21gr and that there was a substantial (1.5- to 3.4-fold) increase in fluorescence intensity per cell (Figure 3). Likewise, similar patterns were observed for many mutants in the nitrogen-deprivation lipid-induction treatment (Figures S2 and S3).

Fatty acid composition

Fatty acid composition was examined in samples collected for lipid contents. The major fatty acids were 16 : 0, 18 : 1, 18 : 2 and 18 : 3, which indicates the composition of 21gr is similar to that reported for several other *C. reinhardtii* strains (James *et al.*, 2011; Siaut *et al.*, 2011). The fatty acid profile of 21gr did not differ between the stationary phase and N-deprivation treatments (Table 1). Based on unsaturated, saturated and polyunsaturated (PUFA) fatty acid composition, we identified three groups of 21gr-derived high-lipid content mutants: (i) those profiles unchanged from the 21gr strain (g8, g30, g31); (ii) those whose fatty acid composition is dependent on N-availability (g35, g9); and (iii) those whose fatty acid composition is different from 21gr and is altered by N-availability (g22, g23). Because mutant g8 has low-starch levels (Figure 2d), it is likely not a sibling of either g30 or g31. The different lipid content patterns of g30 and g31 also suggest that they are not siblings (Figure 2a,b). Similarly, g9 is likely not a sibling of g35 since it exhibits a distinct lipid content and biomass yield pattern than g35. Given these differences in lipid content, biomass yields and fatty acid profiles of the characterized strains, collectively, the data indicate we isolated seven distinct 21gr-derived lipid hyperaccumulating mutants.

Lipid hyperaccumulating mutants derived from a low-starch mutant

Given that low-starch *C. reinhardtii* strains accumulate more lipids (James *et al.*, 2011; Li *et al.*, 2010), we used our FACS-based procedure to isolate mutants in an existing low-starch strain with the aim of producing even more lipids in this already high-lipid-producing strain. We generated the low-starch accumulating strain 21st1 by crossing the 21gr strain with the low-starch strain CC2686 (*mt*$^-$ *sta1-1 nit1 nit2*), which lacks the ADP-glucose pyrophosphorylase large subunit (Van den Koo-

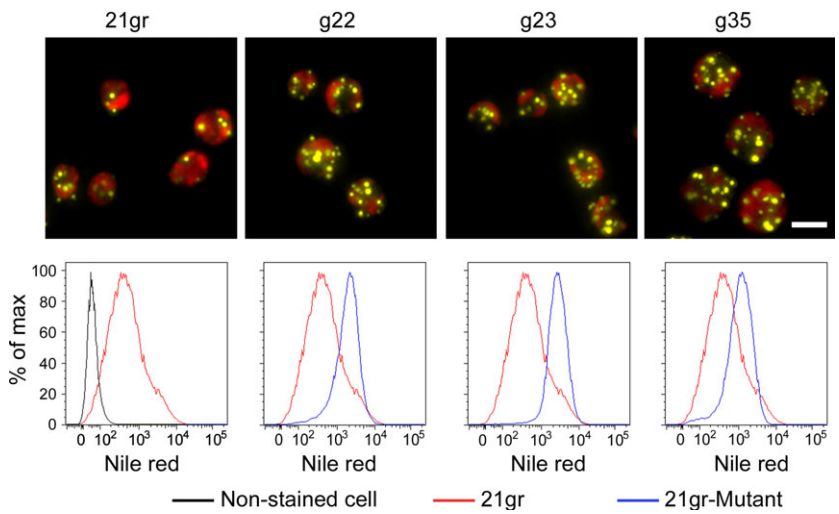

Figure 3 Visualization of Nile Red stained lipid bodies and flow cytometry analysis of Nile Red fluorescence intensities of stained cells of 21gr and its lipid hyperaccumulating mutants. Top, Photomicrographs of Nile Red stained 21gr and selected lipid hyperaccumulating mutants 36 h after the onset of stationary phase. Cells were grown as described in the legend of Figure 2. Yellow fluorescence observed in the presence of Nile Red indicates the presence of neutral lipid while the red fluorescence corresponds to chlorophyll autofluorescence. Bar, 10 μm. Lower, Histogram showing the distribution of Nile Red fluorescence intensity per cell of the same cultures used for visualizing lipid bodies. All nonstained 21gr and mutants exhibit low levels of fluorescence intensities as illustrated with 21gr (Black line). Red line: fluorescence intensity of Nile Red stained 21gr; Blue line: fluorescence intensity of Nile Red stained mutant.

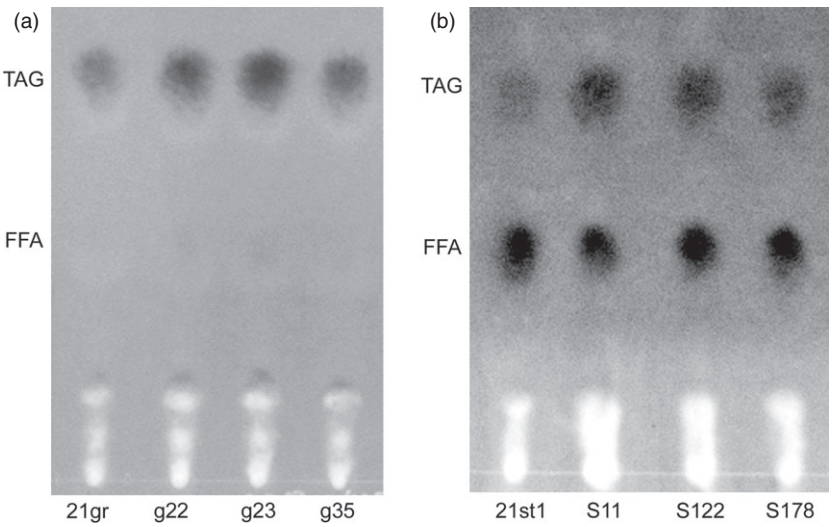

Figure 4 TLC analysis of representative lipid hyperaccumulating 21gr- (a) and 21st1-derived (b) illustrating increased triacylglycerol accumulation by mutant strains. Lipids were isolated from stationary phase (a) and 5 mM urea-N (b) treatments. Lipids were spotted on an equal dry weight basis.

Table 1 Fatty acid composition of representative 21gr mutants

	% Fatty acid, Mean ± SE (n = 3)							
Fatty acid	21gr S	g8 S	g22 S	g31 S	g30 S	g9 S	g35 S	g23 S
16 : 0	22.7 ± 1.2	21.4 ± 2.6	22.0 ± 2.6	23.2 ± 2.3	24.3 ± 0.7	23.3 ± 0.4	24.7 ± 0.8	21.9 ± 0.04
16 : 1 ω9c	6.1 ± 0.5	6.2 ± 0.3	**4.1 ± 1.2**	5.4 ± 0.1	5.8 ± 0.0	6.9 ± 0.0	5.4 ± 0.1	7.0 ± 0.03
18 : 0	3.6 ± 0.4	3.1 ± 0.3	**7.6 ± 2.1**	3.4 ± 0.3	3.6 ± 0.3	3.4 ± 0.1	3.1 ± 0.2	3.0 ± 0.1
18 : 1 ω7c	15.9 ± 0.8	**18.8 ± 0.5**	16.8 ± 0.3	**20.0 ± 1.7**	16.6 ± 0.5	**19.5 ± 1.0**	17.3 ± 0.8	16.4 ± 0.3
18 : 1 ω9c	14.9 ± 1.8	12.9 ± 1.1	**8.4 ± 2.4**	**9.1 ± 0.9**	13.6 ± 0.2	14.1 ± 0.4	13.6 ± 0.3	14.6 ± 0.3
18 : 2 ω6,9c	8.6 ± 1.1	7.2 ± 0.1	7.4 ± 2.6	9.4 ± 0.6	9.8 ± 0.8	9.7 ± 0.3	10.2 ± 0.5	**12.7 ± 0.1**
18 : 3(5,9,12)	6.8 ± 0.4	6.1 ± 0.4	**4.7 ± 1.3**	7.5 ± 0.5	6.8 ± 0.3	5.8 ± 0.4	6.9 ± 0.0	6.5 ± 0.3
Saturated	27.6 ± 1.5	25.9 ± 2.2	**31.8 ± 0.1**	27.9 ± 2.6	29.2 ± 0.5	28.1 ± 0.4	28.9 ± 1.1	26.1 ± 0.05
PUFA	15.4 ± 1.4	13.3 ± 0.5	12.2 ± 3.9	16.9 ± 1.0	16.6 ± 1.1	15.4 ± 0.8	17.0 ± 0.5	**19.2 ± 0.4**
Unsaturated	53.4 ± 2.0	51.5 ± 0.7	**41.7 ± 8.0**	51.7 ± 1.9	50.3 ± 1.8	56.0 ± 1.8	53.5 ± 0.1	57.3 ± 0.4
Saturated/Unsaturated	0.5 ± 0.04	0.5 ± 0.04	**0.8 ± 0.1**	0.5 ± 0.05	0.6 ± 0.03	0.5 ± 0.02	0.5 ± 0.02	0.5 ± 0.00
	21gr -N	g8 -N	g22 -N	g31 -N	g30 -N	g9 -N	g35 -N	g23 -N
16 : 0	24.4 ± 0.2	23.2 ± 2.5	24.8 ± 1.4	**25.9 ± 0.1**	25.0 ± 1.0	25.3 ± 1.3	**25.9 ± 0.6**	24.2 ± 0.8
16 : 1 ω9c	5.0 ± 0.2	4.6 ± 2.0	5.1 ± 0.2	5.5 ± 1.6	5.8 ± 0.7	5.0 ± 0.2	4.5 ± 1.1	**6.2 ± 0.3**
18 : 0	3.6 ± 0.3	**2.7 ± 0.2**	3.4 ± 0.3	3.7 ± 0.2	4.0 ± 0.6	4.5 ± 0.7	4.4 ± 0.7	3.2 ± 0.03
18 : 1 ω7c	16.0 ± 0.3	**18.2 ± 1.0**	17.5 ± 0.7	17.7 ± 0.9	17.5 ± 1.1	16.0 ± 0.4	**17.5 ± 0.4**	15.6 ± 0.8
18 : 1 ω9c	14.9 ± 1.7	13.3 ± 1.5	**10.6 ± 1.1**	12.6 ± 1.2	13.4 ± 1.6	13.0 ± 1.0	13.9 ± 0.8	15.4 ± 1.1
18 : 2 ω6,9c	8.1 ± 0.7	7.8 ± 1.2	**12.4 ± 0.6**	**10.1 ± 0.9**	**11.0 ± 1.1**	9.7 ± 0.7	9.1 ± 1.2	**12.4 ± 0.8**
18 : 3(5,9,12)	6.6 ± 0.3	6.5 ± 0.4	7.1 ± 0.8	6.3 ± 0.8	6.7 ± 0.6	**5.1 ± 0.5**	6.3 ± 0.7	6.8 ± 0.4
Saturated	29.3 ± 0.5	27.2 ± 2.6	29.3 ± 1.5	30.7 ± 0.3	30.3 ± 1.4	31.4 ± 1.8	31.7 ± 1.0	28.5 ± 0.6
PUFA	14.7 ± 0.9	14.2 ± 1.6	**19.5 ± 0.2**	16.3 ± 1.4	17.7 ± 1.5	14.8 ± 0.9	15.4 ± 1.8	**19.2 ± 0.4**
Unsaturated	50.9 ± 0.7	50.5 ± 0.1	50.6 ± 4.5	52.2 ± 2.5	54.6 ± 2.4	47.4 ± 3.0	49.9 ± 0.4	**56.6 ± 1.0**
Saturated/Unsaturated	0.58 ± 0.02	0.54 ± 0.05	0.58 ± 0.02	0.59 ± 0.02	0.56 ± 0.05	**0.67 ± 0.07**	**0.64 ± 0.01**	0.50 ± 0.02

PUFA, polyunsaturated fatty acids; Saturated/Unsaturated, saturated/unsaturated fatty acid ratio.

Cells were harvested 36 h after the onset of stationary phase (S) or N-deprivation (-N) treatment. Values in bold are statistically different from 21gr based on a two-sided t-test ($P < 0.05$). Only fatty acids >2.0% are included in this table.

rnhuyse *et al.*, 1996; Zabawinski *et al.*, 2001). As compared to the 21gr, strain 21st1 contains approximately 20% of the starch and 144–176% of the lipid content of the former (Table S2). The resulting strains were evaluated in a newly developed flask-based system that increased throughput and restricted the FACS sorting gate further to reduce the number of mutants to screen.

The EMS mutagenesis kill rate with strain 21st1 was 94%, and following recovery and nitrogen-deprivation induction period, we subjected 7×10^8 cells to FACS. In this sorting, 0.02% of the cells exhibited Nile Red fluorescence intensities in the sorting gate optimized for extremely high Nile Red Fluorescence (Figure 1b). The inherently high Nile Red fluorescence of the parental 21st1

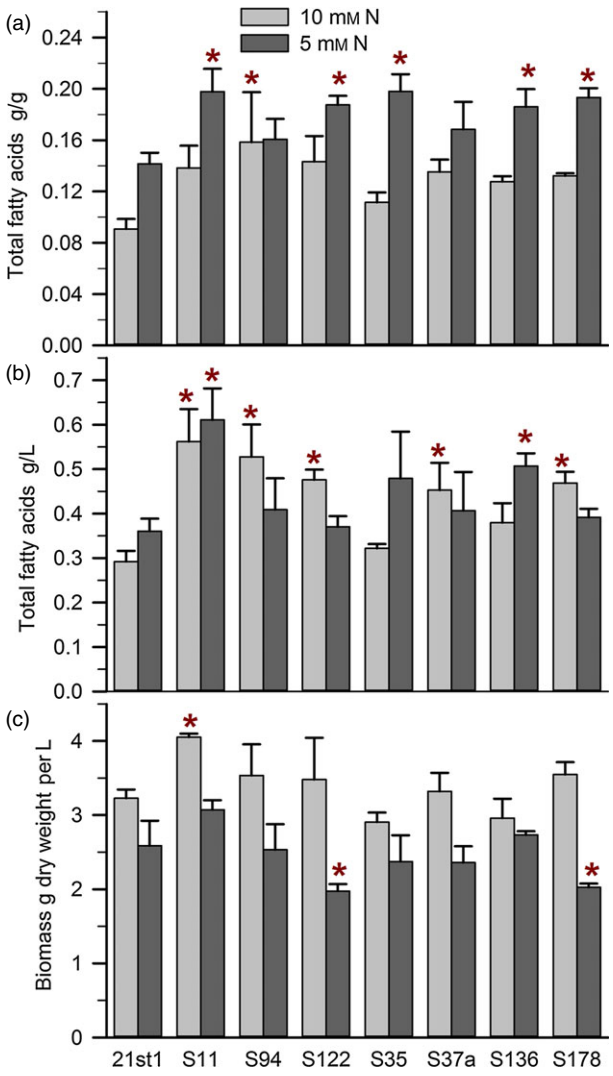

Figure 5 Lipid contents (a) and yields (b) and biomass yields (c) of 21st1 mutants. Data are means ± SE from three independent assays. Biomass values for lipid analyses were obtained 48 h after the onset of stationary phase in 10 mM urea-N (open bars) and 5 mM urea-N (closed bars). Separate ANOVAs were performed for the 5 and 10 mM urea concentrations and asterisks above bars indicate values are statistically different from progenitor 21st1 based on a student's *t*-test ($P < 0.05$).

colonies precluded the use of the Nile Red bright colony phenotype to visually identify putative 21st1 lipid hyperaccumulating mutants. Consequently, we screened all 133 recovered mutants for lipid content in flask bioreactors with 10 or 5 mM urea in a 5% CO_2 atmosphere. We reasoned that the lower N-concentration would simulate the effect of an N-deprivation treatment, with less manipulation of the culture. Our results (Figure 5a) show that this is indeed the case; the 5 mM urea-N treatment resulted in statistically ($P < 0.05$) higher 21st1 lipid yields than the 10 mM urea–N treatment. In our pipeline, each mutant was cultivated without replication and rescreened only if lipid content was at least 10% greater than 21st1. From these analyses, we identified three mutant classes with increased lipid content (g lipid/g dry weight biomass): (i) in both the 5 and 10 mM urea ($n = 4$); (ii) only in the 10 mM urea ($n = 1$); and (iii) only in the 5 mM urea ($n = 1$) treatments (Figure 5). Lipid contents in the 5 and 10 mM urea–N treatments were 31–40% and 40–58% greater than the parental 21st1 strain. Lipid yields on a per culture volume basis (Figure 5b) were greatly influenced by biomass yields (Figure 5c), most notably the statistically significant 26% increase in biomass of mutant S11 in the 10 mM urea–N treatment and the reduced biomass of S122 and S178 with 5 mM urea. Consequently, mutant S11 exhibited a 69–92% increase in lipid yields in the 5 and 10 mM urea–N treatments (Figure 5b).

As shown visually and quantitatively (Figure 6), 21st1-derived lipid hyperaccumulating mutants contained more lipid bodies than 21st1, and increased Nile Red fluorescence is positively correlated with TAG accumulation as determined by TLC analysis in the 5 mM treatment (Figure 4). Unlike 21gr-derived mutants (Figure 3), there was a bimodal Nile Red staining pattern in the 21st1-derived mutants; one subpopulation exhibited 21st1-level fluorescence intensities, and the other subpopulation exhibited a substantial (4- to 11-fold) increase in fluorescence intensity per cell (Figure 6). In the 10 mM urea–N treatments, the TLC (Figure S2b) and Nile Red staining (Figure S3b) results were congruent with the total lipid yields (Figure 5), indicating that this condition was not conducive to lipid accumulation.

Fatty acid composition of 21st1 mutants

Fatty acid composition was examined in the 5 and 10 mM urea–N treatment samples collected for lipid contents. Whole cell fatty acid composition of 21gr and 21st1 do not differ substantially, with a few exceptions (compare Tables 1 and 2), while N-availability had a strong impact on the 21st1 profile with a shift towards more PUFA and saturated fatty acids in the 5 mM compared with the 10 mM N treatments (Table 2). Based on the unsaturated, saturated and PUFA compositions, we identified three groups of 21st1 hyperlipid accumulating mutants: (i) those with wild-type fatty acid composition (S94); (ii) those whose fatty acid composition is N-availability dependent (S35, S37a, S136); and (iii) those whose fatty acid composition is different from 21st1 and N-availability dependent (S11, S178). Because mutant S11 is a high-biomass strain (Figure 5c), it is likely not a sibling of S178. Similarly, S136 is likely not a sibling of S37a and S35, who exhibit distinct lipid accumulation patterns from not only S136 but also from each other (Figure 5a,b). Given the differences in lipid content, biomass yields, and whole fatty acid profiles, collectively, the data imply that we isolated six distinct 21st1-derived lipid hyperaccumulating mutants.

Discussion

Here, we report the utility of FACS sorting of Nile Red fluorescence stained *C. reinhardtii* cells to isolate mutants that hyperaccumulate lipids. We capitalized on previous studies with various wild microalgae (Doan and Obbard, 2012; Hyka *et al.*, 2013; Montero *et al.*, 2011) to develop a robust Nile Red staining, FACS, and mutant phenotype characterization pipeline to efficiently isolate mutants that hyperaccumulate lipids. These mutants will provide a rich genetic resource for understanding the molecular and genetic mechanisms contributing to repartitioning cellular resources into high-lipid-yielding strains without sacrificing starch accumulation. Our results also illustrate the feasibility of stacking desired traits onto already high-lipid producing strains to further increase lipid content. Importantly, our results suggest that enhancing lipid content can be achieved without manipulating bioreactors to impose a nutrient stress, which is typically

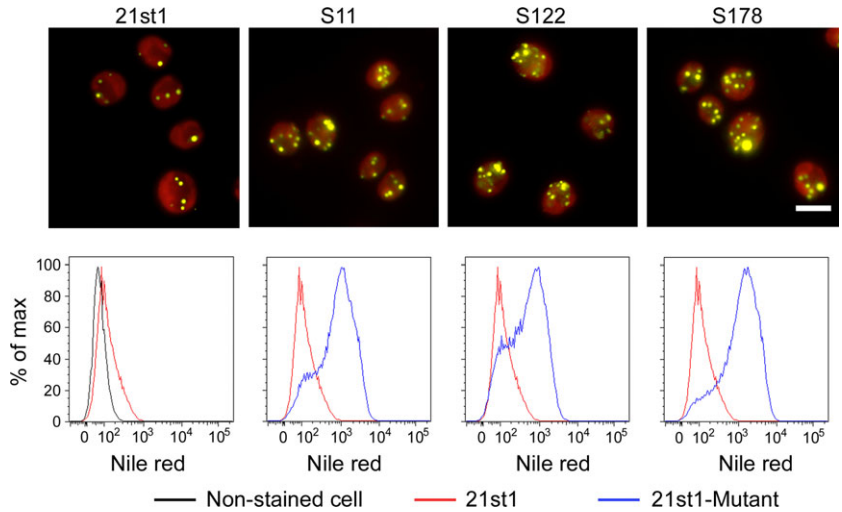

Figure 6 Visualization of Nile Red stained lipid bodies and flow cytometry analysis of Nile Red fluorescence intensities of stained cells of 21st1 and its lipid hyperaccumulating mutants. Top, Photomicrographs of Nile Red stained 21st1and selected lipid hyperaccumulating mutants grown in 5 mM urea-N 48 h after the onset of stationary phase. Cells were grown as described in the legend of Figure 5. Yellow fluorescence observed in the presence of Nile Red indicates the presence of neutral lipid while the red fluorescence corresponds to chlorophyll autofluorescence. Bar, 10 μm. Lower, Histogram showing the distribution of Nile Red fluorescence intensity per cell of the same cultures used for visualizing lipid bodies. All nonstained 21st1 and mutants exhibit low levels of fluorescence intensities as illustrated with 21st1 (Black dashed-line). Red line: fluorescence intensity of Nile Red stained 21st1; Blue line: fluorescence intensity of Nile Red stained 21st1-derived mutant cells.

Table 2 Fatty acid profiles of 21st1 mutants

	% Fatty acid, Mean ± SE (n = 3)							
Fatty acid	21st1 10-N	S11 10-N	S94 10-N	S122 10-N	S35 10-N	S37a 10-N	S13610-N	S178 10-N
16 : 0	16.5 ± 0.3	19.3 ± 2.9	16.5 ± 1.0	19.3 ± 1.2	15.8 ± 0.7	21.8 ± 2.8	16.4 ± 0.9	18.5 ± 1.6
16 : 1 ω9c	6.7 ± 0.3	5.9 ± 1.1	4.2 ± 2.0	5.7 ± 1.1	7.8 ± 0.7	5.4 ± 0.9	7.3 ± 0.7	7.3 ± 0.5
18 : 0	2.6 ± 0.5	5.2 ± 1.7	4.7 ± 1.6	5.1 ± 2.9	1.8 ± 0.2	2.1 ± 0.2	1.9 ± 0.1	2.4 ± 0.1
18 : 1 ω7c	18.3 ± 1.3	13.9 ± 2.4	19.8 ± 3.2	15.1 ± 0.6	18.7 ± 0.6	17.3 ± 2.4	17.1 ± 1.1	**15.2 ± 1.1**
18 : 1 ω9c	11.2 ± 0.8	12.5 ± 2.1	11.7 ± 0.8	13.0 ± 1.6	12.8 ± 1.3	11.0 ± 1.8	13.0 ± 1.7	**15.1 ± 0.9**
18 : 2 ω6,9c	8.1 ± 0.2	6.6 ± 1.7	8.4 ± 0.9	9.2 ± 2.6	7.5 ± 0.5	8.5 ± 1.5	9.4 ± 0.9	12.3 ± 0.4
18 : 3(5,9,12)	4.5 ± 0.1	3.8 ± 0.8	4.3 ± 0.7	4.0 ± 0.7	4.3 ± 0.1	4.4 ± 0.2	4.4 ± 0.2	4.4 ± 0.1
Saturated	20.9 ± 1.0	**26.6 ± 2.7**	23.1 ± 1.1	**26.1 ± 2.4**	19.0 ± 1.1	25.1 ± 3.0	19.6 ± 0.9	22.1 ± 1.6
PUFA	12.6 ± 0.3	10.3 ± 2.4	12.7 ± 1.6	13.1 ± 3.3	11.8 ± 0.5	16.6 ± 3.6	13.8 ± 0.9	**16.6 ± 0.4**
Unsaturated	49.2 ± 0.9	42.9 ± 4.9	45.3 ± 4.0	47.1 ± 5.9	51.5 ± 1.0	50.5 ± 0.2	51.5 ± 1.4	**54.4 ± 1.5**
Saturated/Unsaturated	0.43 ± 0.03	**0.64 ± 0.1**	0.52 ± 0.08	0.6 ± 0.1	0.37 ± 0.03	0.50 ± 0.06	0.38 ± 0.01	0.41 ± 0.04
Fatty acid	21st1 5-N	S11 5-N	S94 5-N	S122 5-N	S35 5-N	S37a 5-N	S136 5-N	S178 5-N
16 : 0	26.0 ± 1.5	27.7 ± 0.5	27.7 ± 1.5	27.5 ± 1.0	26.1 ± 0.6	27.6 ± 1.2	26.8 ± 0.6	27.5 ± 0.8
16 : 1 ω9c	4.3 ± 0.5	5.0 ± 0.1	4.0 ± 0.2	4.2 ± 0.3	5.7 ± 0.6	4.0 ± 1.2	5.0 ± 0.5	4.3 ± 0.3
18 : 0	3.1 ± 0.4	3.0 ± 0.1	3.1 ± 0.4	2.9 ± 0.0	2.4 ± 0.4	2.9 ± 0.4	2.5 ± 0.1	2.8 ± 0.1
18 : 1 ω7c	14.3 ± 0.5	13.3 ± 0.2	13.4 ± 0.4	**13.0 ± 0.4**	**13.0 ± 0.2**	14.8 ± 0.7	**12.5 ± 0.3**	13.1 ± 0.2
18 : 1 ω9c	11.3 ± 1.3	13.8 ± 0.1	13.5 ± 1.7	13.2 ± 1.4	**17.7 ± 0.7**	13.7 ± 0.4	**15.5 ± 1.3**	12.6 ± 0.5
18 : 2 ω6,9c	12.8 ± 0.6	**16.3 ± 0.2**	14.1 ± 2.2	14.8 ± 1.9	12.2 ± 0.7	12.9 ± 1.4	13.7 ± 1.2	16.6 ± 0.6
18 : 3(5,9,12)	5.1 ± 0.1	**4.5 ± 0.0**	4.8 ± 0.6	5.1 ± 0.3	4.6 ± 0.2	4.7 ± 0.2	4.7 ± 0.2	5.1 ± 0.2
Saturated	30.6 ± 1.9	31.8 ± 0.7	29.5 ± 3.6	31.6 ± 0.9	29.4 ± 1.0	31.7 ± 1.6	30.3 ± 0.9	31.3 ± 0.8
PUFA	17.8 ± 0.5	**20.7 ± 0.2**	18.9 ± 2.9	19.9 ± 2.2	16.8 ± 0.5	17.6 ± 1.5	18.4 ± 1.3	21.8 ± 0.8
Unsaturated	48.0 ± 1.0	**53.0 ± 0.3**	50.1 ± 1.0	**50.5 ± 0.7**	**53.4 ± 0.5**	**50.4 ± 1.7**	**51.6 ± 1.0**	**51.8 ± 0.2**
Saturated/Unsaturated	0.64 ± 0.05	0.6 ± 0.02	0.64 ± 0.0	0.6 ± 0.01	0.55 ± 0.02	0.63 ± 0.05	0.6 ± 0.03	0.6 ± 0.01

PUFA, polyunsaturated fatty acids; Saturated/Unsaturated, saturated/unsaturated fatty acid ratio.

Cells were harvested 48 h after the onset of stationary phase in 10 (10-N) or 5 (5-N) mM urea cultures. Values in bold are statistically different from 21st1 based on a two-sided t-test ($P < 0.05$). Only fatty acids >2.0% are included in this table.

the case for the reported increases in lipid content of starchless *C. reinhardtii* strains. There is clearly a cost to N-stress, particularly in starch-deficient strains since biomass reductions (Figure 5b) decrease bioreactor yields.

By combining lipid content, biomass yields and fatty acid profile analyses, we determined that we isolated a variety of distinct mutants. Given the nature of our screen, these mutants may be particularly adept at accumulating lipids after relatively short N-deprivation or stationary phase lipid-induction periods. At present, we do not know whether high-lipid contents of these mutants are attained during vegetative growth or whether longer lipid-induction periods would further increase lipid yields. Of particular interest are the high-lipid content and high-biomass yielding strains (g9 and S11; Figures 2 and 5). It will be worthwhile determining if the high lipid and high-biomass phenotypes are linked or due to separate mutations. On a dry weight basis several 21gr-derived lipid hyperaccumulating mutants with wild-type starch levels accumulated as much neutral lipid as the low-starch derivative 21st1, and the difference between 21gr-derived mutants and 21st1 is further highlighted because the poorer biomass yields of low-starch mutants substantially decreased lipid yields (e.g. g9 or g30; compare Figure 2 with Table S2). This significant finding demonstrates that substantial increases in lipid content can be attained other than by repartitioning carbon from starch to lipid production (Figure 2). This potentially has broad implications on strategies for metabolic engineering algae to increase lipid yields and productivity, particularly if the length of lipid-inductions periods can be reduced.

We also demonstrated that it is possible to stack mutations onto strains to further increase lipid content. Our approach was to first construct a low-starch accumulating strain by crossing 21gr with the low-starch strain CC2686 (*mt⁻ sta1-1 nit1 nit2*) that lacks the ADP-glucose pyrophosphorylase large subunit (Zabawinski *et al.*, 2001), generating strain 21st1. Neutral lipid content of 21st1 is consistent with reports with other low-starch strains (Siaut *et al.*, 2011; Wang *et al.*, 2009): high-level lipid content particularly following nitrogen stress (Table S2 and Figure 5). Moreover, our ability to isolate 21st1-derived mutants with lipid contents 31–58% greater than 21st1 clearly indicates the potential for stacking desirable traits to further increase lipid content.

Compared to their progenitors, increased total fatty acid content (Figures 2 and 5) of some 21gr- and 21st1-derived mutants correlates with increased number of lipid bodies (Figures 3 and 6) and in TAG accumulation (Figure 4). Some lipid bodies of the mutants appear to be larger than the progenitor, but the increase in lipid body size is not as substantial as reported recently for several other low-starch *C. reinhardtii* strains (James *et al.*, 2011; Li *et al.*, 2010). These differences are likely the consequence of differences in cultivation medium and other growth parameters. Also, longer lipid-induction periods in these other studies may have resulted in greater differences in lipid body sizes.

The overall fatty acid composition remained relatively constant across each progenitor strain and its corresponding lipid hyperaccumulating mutants. Differences in fatty acid profiles were typically mutant specific. The exception is the slightly higher proportion of unsaturated fatty acids in 21st1-derived mutants compared with 21st1 in the 5 mM urea treatment (Table 2). Biodiesel feedstock requires that the PUFA content be low, and our whole cell fatty acid analysis indicated that most of the 21gr- and 21st1-derived lipid hyperaccumulating mutants exhibited progenitor PUFA levels (Tables 1 and 2).

The flexibility enabled by controlling the FACS sorting gate permitted restricting the number of mutants screened for lipid content verification. Despite this advantage, it is not uncommon to rely on a post-FACS Nile Red staining procedure to validate high Nile Red fluorescence of sorted cells (Cagnon *et al.*, 2013; Doan and Obbard, 2012). One approach is to screen mutants for elevated Nile Red staining in liquid culture, which is time-consuming. Our data indicate that incorporating Nile Red into solid media is a faster and more robust approach for validating high Nile Red fluorescence, and presumably high-lipid content mutants than repeatedly rescreening individual isolates in liquid media even in a high-throughput manner. In our study, 30% of the mutants exhibiting a Nile Red bright colony phenotype had lipid yields 10% greater than the progenitor in every analysis. In contrast, only 1.3% of the mutants exhibiting a non-Nile Red bright colony phenotype had sufficiently high Nile Red fluorescence in liquid culture to warrant lipid yield validation: even fewer accumulated more lipids. The inherently high Nile Red fluorescence of the low-starch strain 21st1 colonies complicated our ability to incorporate the Nile Red bright colony phenotype into this mutant verification pipeline. This could be overcome by incorporating other image analysis tools, such as charge-couple devices, that measure fluorescence intensity to facilitate differentiating fluorescence intensity of colonies.

Our approach relying solely on a hyperfluorescence FACS gate can efficiently screen a large population of putative mutants in a timely manner. For example, we sorted 133 putative 21st1-derived mutants and validated 24 lipid hyperaccumulating mutants within 3 weeks, which is an 18% success rate. This screen without additional FACS or microtitre-plate confirmatory steps is more efficient than our experiment with 21gr and other studies relying on additional Nile Red staining confirmatory steps (Cagnon *et al.*, 2013; Doan and Obbard, 2012). There are several possible explanations for why we did not observe near 100% correlation (i.e. lower false positives in the FACS step) between the high Nile Red fluorescence signal in the FACS and validation of lipid content. The most significant factor influencing our success rate was our criterion that for a putative lipid hyperaccumulating mutant to be retained in our pipeline lipid yields needed to be 10% greater than the parental strain, which inherently decreased our success rate. We selected this strict criterion to identify high yielding mutants, because we wanted to identify mutants with large rather than small increases in lipid yield. Additional factors influencing our success rate could include as follows: (i) mistakes during sorting due too fast flow speeds or multicellular aggregates with high fluorescence signals; (ii) because the broad bandpass of the FACS filter detected other Nile Red stained hydrophobic macromolecules (Pinzon *et al.*, 2011); (iii) inherent biological variability in neutral lipid production due to differences in cultivation. Consequently, greater efficiency could be obtained by further optimizations of FACS procedures, Nile Red staining and synchronization of uniform physiological states in different aspects of the screen.

In conclusion, we describe a high-throughput procedure for isolating lipid hyperaccumulating mutants of *C. reinhardtii* and demonstrate its effectiveness with two strains with inherently different neutral lipid accumulation capabilities. By coupling FACS sorting of high Nile Red fluorescence stained cells with a rapid, lipid screening procedure a rich resource of strains were obtained. Significantly our approach shows that nitrogen-starvation is not

necessary for attaining high-lipid yields, you can increase lipid yields by stacking mutations on top of already high-lipid-yielding low-starch strains, and that another route for increasing productivity is with high-biomass mutants. The mutants will also enable understanding the molecular and genetic mechanisms contributing to repartition of cellular resources into high-lipid-yielding strains without sacrificing starch accumulation.

Experimental procedures

Strains

The *C. reinhardtii* wild-type 21gr (CC1690) and low-starch mutant CC2686 (*mt⁻ sta1-1 nit1 nit2*) strains were obtained from the *Chlamydomonas* Stock Center, the University of Minnesota, St. Paul, MN. The *sta1* mutant CC2686, lacks the ADP-glucose pyrophosphorylase large subunit and contains approximately 5–10% of wild-type starch levels (Van den Koornhuyse *et al.*, 1996). The *sta1* strain was crossed to 21gr following techniques described by Harris (Harris, 2009). Random progeny were selected on TAP plates (Gorman and Levine, 1965) containing nitrate as the sole nitrogen source. Iodine staining identified low-starch containing progeny one of which, designated 21st1 (*mt⁻ sta1-1 NIT1 NIT2*), was used for the experiments described in this report.

Media and growth conditions

For characterization of progenitor and mutant phenotypes, strains were cultivated in a modified minimal medium (MM) in which 10 mM or 5 mM urea replaced NH_4NO_3 (Geraghty *et al.*, 1990). Wild-type 21gr and its mutants were grown photoautotrophically in 35 mm × 300 mm glass tubes (Corning, Corning, NY) converted for use as PBRs. The tube screw-caps were modified to contain a stainless steel tube spanning the full length of the tube to bubble gas through a stainless steel airstone at the base of the culture tube. The cap also contained a second port for a 20G × 8 inch syringe needle for culture sampling. A third port contained a filtered tube that functioned as an exhaust for effluent gas. Cultures were aerated through the airstone with a sterile filtered gas mixture of 5% CO_2 in air at approximately 50 mL/min, which also mixed the culture. The PBRs were arranged in two rows of eight in a 10-gallon acrylic aquarium, 50.8 cm × 25.4 cm × 30.5 cm, which was filled with water maintained at 25 °C with a recirculating refrigerated water bath. Cultures were under a constant illumination of 350–500 μE/m/s (as measured from the center of the culture tube) from daylight fluorescent lights placed lengthwise immediately adjacent to the opposing sides of the aquarium. Cultures were grown in 200 mL of MM medium with 10^5 cells mL inoculum. Growth was monitored by measuring culture absorbance (OD_{750}). The nitrogen-starvation treatment consisted of pelleting cells by centrifugation when they reached stationary phase, and re-suspending the cells in nitrogen-free MM medium and cultivating in PBRs for an additional 36 h as described above. Preliminary data indicated there was no difference in total lipid contents for nitrogen-deprivation treatments between 24 and 48 h in length. The low-starch strain 21st1 and mutants derived thereof were grown photoautotrophically under continuous illumination (120 μE/m^2/s) for 5 days at 25 °C in 25 mL MM in a New Brunswick orbital shaker fitted with a plastic box to maintain the targeted 5% CO_2 atmosphere. Biomass from the entire reactor volume was collected by centrifugation and then freeze dried prior to lipid analyses.

EMS mutagenesis

Both 21gr and 21st1 were grown in 40 mL MM bubbled with 5% CO_2 at 25 °C under continuous illumination (120 μE/m^2/s) for 3 days to reach early stationary phase (10^7 cells/mL density). Cells were pelleted by centrifugation and resuspended in MM containing 300 mM EMS (Sigma-Aldrich, St. Louis, MO) for 80 min. Cells were then washed thrice with MM to remove residual EMS and re-suspended in fresh MM medium and allowed to recover for 12 h in the dark. Prior to flow sorting, cultures were incubated in nitrogen-free MM for 36 h to stimulate TAG accumulation as described above.

Fluorescence-activated cell sorting

Cells were stained with 0.5 μg/mL Nile Red [50 μg/mL stock in DMSO; (Chen *et al.*, 2009)] for 10 min in the dark prior to flow sorting with a BD FACSAria III at the Iowa State University Flow Cytometry Facility. The 488 nm argon laser was used to excite Nile Red and chlorophyll fluorescence which were detected at 570 ± 26 nm (PE-A channel) and 695 ± 45 nm (PerCp-Cy5-5A channel), respectively. Dot plots of chlorophyll and Nile Red fluorescence intensities of the 21gr cells were used to establish gates for isolating putative lipid hyperaccumulating mutants with Nile Red fluorescence intensities > 99.99% of the population. A similar gating strategy was used for mutants derived from 21st1 but we narrowed the gate further, requiring putative lipid hyperaccumulating mutants to exhibit fluorescence intensities >99.999% of the cell population (see Figure 1). Recovery of 21gr- and 21st1-derived mutants detected in the sorting gate was 3.3% and 0.14%, respectively. The sorted cells were collected in MM with acetate and immediately plated onto MM medium amended with 1.5% agar containing 0.5 μg/mL Nile Red. Plates were incubated at 25 °C in 5% CO_2 atmosphere and an illumination intensity of 120 μE/m^2/s. After 1 week colonies were examined under an epi-fluorescence microscope to identify mutants exhibiting Nile Red fluorescence intensities greater than wild-type 21gr. These were referred to as Nile Red bright colony mutants and presumably would be lipid hyperaccumulating mutants.

Liquid culture Nile Red fluorescence screen

Colonies of 21gr and putative lipid hyperaccumulating mutants grown on MM plates were aseptically transferred into 48-well culture plates containing 800 μL MM or N-free MM for 3 days prior to Nile Red staining as described above. We used a fluorescence plate reader (EX: 530 ± 25; EM: 590 ± 35; Synergy HT, Winooski, VT) to measure Nile Red fluorescence which was normalized to culture biomass (OD_{750}). Mutants that repeatedly exhibited Nile Red fluorescence 1.5-fold greater than the parental strain 21gr in three independent screens were considered candidates for further lipid analysis.

TAG detection and fatty acid quantification

For characterization of TAG accumulation, total lipids were extracted from lyophilized cells using a chloroform–methanol–water extraction procedure described previously (Bligh and Dyer, 1959). Lipids were spotted onto the silica plates on an equivalent biomass (g dry weight) basis. Neutral lipids were separated on 200-μm-thick silica plates (Fluka, St. Louis, MO) by thin layer chromatography using a hexane/diethyl ether/acetic acid (70 : 30 : 2, by volume) solvent. The silica plates were sprayed with a 0.05% primulin (Direct Yellow 59) solution in acetone and

water (8 : 2, v/v) as described previously (White *et al.*, 1998) and after drying the TAG band was visualized under UV-illumination. For total lipid analysis, 10 mg of lyophilized cells were spiked with 10 μg of an internal standard [C19:0; nonadecanoid acid (Sigma-Aldrich)]. Fatty acid methyl esters were generated according to a modified version of a previously described protocol (Bonaventure *et al.*, 2003). Lyophilized cell pellets were heated at 110 °C for 24 h in 500 μL 10% (w/v) aqueous $Ba(OH)_2$ (Sigma-Aldrich) and 550 μL 1,4-dioxane (Sigma-Aldrich). After heating, the solution was acidified to pH <4 with 6 N HCl. Fatty acids were extracted twice with 2 mL hexane, and the pooled extract was evaporated to dryness with a N_2 gas stream. Fatty acids were methylated by adding 2 mL 1 N HCl in methanol and heating at 80 °C for 1 h. After methylation, 2 mL of 0.9% NaCl (aqueous) was added and FAMEs were twice extracted with hexane and concentrated under N_2 for analysis by gas liquid chromatography with a flame ionization detector on an Ultra-2 capillary column. Peaks were compared to known standards with the Sherlock-MIDI (Newark, DE) identification system using the Rapid calibration and operating conditions, which requires only 5.3 min for sample analysis. The Sherlock Rapid method was unable to resolve by retention time the 16 : 2 and 16 : 3 fatty acids that were identified by GC-MS (Table S3 and described below), which accounted for 4–9% of the whole cell fatty acid pool.

A subset of samples was analyzed by GC-MS at the WM Keck Metabolomics Research Laboratory, to validate retention time--based FAME identity for comparing FAME profiles of mutants and progenitor strains. GC-MS was performed on an Agilent 6890N gas chromatograph interfaced to a 5973 MSD detector (Agilent Technologies, Santa Clara, CA). The column used was a HP-5 ms (30 m × 0.25 mm, 0.25 mm film thickness; Agilent Technologies). The oven temperature was set to 100 °C for 1 min before ramping at 10 °C/min until reaching a temperature of 260 °C, which was maintained for 5 min, and then the temperature increased 15 °C/min until reaching a final temperature of 320 °C. Helium carrier gas was used at a rate of 1.2 mL/min, and ionization voltage was set to 70 eV.

Starch assay

Starch was extracted from 2 to 10 × 10^6 cells essentially as described previously (Fan *et al.*, 2012). After the extraction, the pH of the starch suspension was adjusted to 4.8 with 1 M acetic acid. The extract was then digested to completion with amyloglucosidase (Sigma-Aldrich). Glucose was then quantified using a commercial glucose assay kit (Sigma-Aldrich).

Microscopy

Epifluoresence microscophs were obtained using a Nikon Eclipse 80i system equipped with a Nikon EZ Coolsnap camera. *Chlamydomonas reinhardtii* chlorophyll auto-fluorescence was visualized using a B2A (EX: 450–480; DM 500; BA515) and Nile Red stained lipid bodies were visualized using a TRITC HYQ filter (EX: 530–560 nm; DM 570 nm; BA: 590–650 nm) filter cube. Superimposed images were created and cropped using Adobe Photoshop.

Flow cytometry

For measuring Nile Red staining of putative lipid hyperaccumulating mutants, we first gated the flow cytometer with 21gr or 21st1 stained with Nile Red to establish a minimum Nile Red fluorescence intensity threshold. Dual-color flow cytometry was performed on a BD FACSCanto flow cytometer at the Iowa State University Cell Facility. The 488-nm argon laser was used to excite chlorophyll, and Nile Red and the 570 ± 26 nm (PE-A channel) and 695 ± 45 nm (PerCp-Cy5-5A channel) were used for the detection of Nile Red and chlorophyll, respectively. Cells were detected in a dot plot of side-scatter versus chlorophyll autofluorescence to ensure that all counted particles were cells. The emission intensities of 10 000–20 000 cells were counted per sample, and the data analyzed with FlowJo software (Tree Star, Inc. Ashland, OR).

Statistical analyses

A separate one-way analysis of variance (ANOVA) was performed for each growth condition to assess whether lipid content or yield, or biomass of mutants were greater than the progenitor strain. Treatment means were compared using a student's *t*-test test ($P < 0.05$). Experiments were comprised of three replications. FAME profiles of mutants were compared to progenitor strains using a two-tailed paired *t*-test ($P < 0.05$). All statistical analyses were performed with JMP (version 10; SAS Institute, Cary, NC).

Acknowledgements

This research was supported by the Department of Energy Advanced Research Program Agency-Energy (DE-AR0000010), the Plant Sciences Institute, and the Iowa Agriculture and Home Economics Experiment Station. We thank Dr. Shawn Rigby for technical assistance with FACS and Shawn Bishop for technical assistance.

References

Beer, L.L., Boyd, E.S., Peters, J.W. and Posewitz, M.C. (2009) Engineering algae for biohydrogen and biofuel production. *Curr. Opin. Biotechnol.* **20**, 264–271.

Bligh, E.G. and Dyer, W.J. (1959) A rapid method of total lipid extraction and purification. *Can. J. Biochem. Physiol.* **37**, 911–917.

Bonaventure, G., Salas, J.J., Pollard, M.R. and Ohlrogge, J.B. (2003) Disruption of the FATB gene in Arabidopsis demonstrates an essential role of saturated fatty acids in plant growth. *Plant Cell*, **15**, 1020–1033.

Boyle, N.R., Page, M.D., Liu, B., Blaby, I.K., Casero, D., Kropat, J., Cokus, S.J., Hong-Hermesdorf, A., Shaw, J., Karpowicz, S.J., Gallaher, S.D., Johnson, S., Benning, C., Pellegrini, M., Grossman, A. and Merchant, S.S. (2012) Three acyltransferases and nitrogen-responsive regulator are implicated in nitrogen starvation-induced triacylglycerol accumulation in *Chlamydomonas*. *J. Biol. Chem.* **287**, 15811–15825.

Cagnon, C., Mirabella, B., Nguyen, H.M., Beyly-Adriano, A., Bouvet, S., Cuine, S., Beisson, F., Peltier, G. and Li-Beisson, Y. (2013) Development of a forward genetic screen to isolate oil mutants in the green microalga *Chlamydomonas reinhardtii*. *Biotechnol. Biofuels*, **6**, 178.

Chen, W., Zhang, C., Song, L., Sommerfeld, M. and Hu, Q. (2009) A high throughput Nile red method for quantitative measurement of neutral lipids in microalgae. *J. Microbiol. Methods*, **77**, 41–47.

Cooksey, K.E., Guckert, J.B., Williams, S.A. and Callis, P.R. (1987) Fluorometric determination of the neutral lipid content of microalgal cells using Nile Red. *J. Microbiol. Methods*, **6**, 333–345.

Doan, T.T.Y. and Obbard, J.P. (2012) Enhanced intracellular lipid in Nannochloropsis sp. via random mutagenesis and flow cytometric cell sorting. *Algal Res.* **1**, 17–21.

Fan, J., Yan, C., Andre, C., Shanklin, J., Schwender, J. and Xu, C. (2012) Oil accumulation is controlled by carbon precursor supply for fatty acid synthesis in *Chlamydomonas reinhardtii*. *Plant Cell Physiol.* **53**, 1380–1390.

Geraghty, A.M., Anderson, J.C. and Spalding, M.H. (1990) A 36 kilodalton limiting-CO(2) induced polypeptide of *Chlamydomonas* is distinct from the 37 kilodalton periplasmic carbonic anhydrase. *Plant Physiol.* **93**, 116–121.

Goodson, C., Roth, R., Wang, Z.T. and Goodenough, U. (2011) Structural correlates of cytoplasmic and chloroplast lipid body synthesis in *Chlamydomonas reinhardtii* and stimulation of lipid body production with acetate boost. *Eukaryot. Cell*, **10**, 1592–1606.

Gorman, D.S. and Levine, R.P. (1965) Cytochrome f and plastocyanin: their sequence in the photosynthetic electron transport chain of *Chlamydomonas reinhardii*. *Proc. Natl Acad. Sci. USA*, **54**, 1665–1669.

Greenspan, P. and Fowler, S.D. (1985) Spectrofluorometric studies of the lipid probe, nile red. *J. Lipid Res.* **26**, 781–789.

Harris, E.H. (ed) (2009) *The Chlamydomonas Sourcebook: Introduction to Chlamydomonas and its Laboratory Use*. Amsterdam; Boston: Elsevier.

Hu, Q., Sommerfeld, M., Jarvis, E., Ghirardi, M., Posewitz, M., Seibert, M. and Darzins, A. (2008) Microalgal triacylglycerols as feedstocks for biofuel production: perspectives and advances. *Plant J.* **54**, 621–639.

Hyka, P., Lickova, S., Přibyl, P., Melzoch, K. and Kovar, K. (2013) Flow cytometry for the development of biotechnological processes with microalgae. *Biotechnol. Adv.* **31**, 2–16.

James, G.O., Hocart, C.H., Hillier, W., Chen, H., Kordbacheh, F., Price, G.D. and Djordjevic, M.A. (2011) Fatty acid profiling of *Chlamydomonas reinhardtii* under nitrogen deprivation. *Bioresour. Technol.* **102**, 3343–3351.

La Russa, M., Bogen, C., Uhmeyer, A., Doebbe, A., Filippone, E., Kruse, O. and Mussgnug, J.H. (2012) Functional analysis of three type-2 DGAT homologue genes for triacylglycerol production in the green microalga *Chlamydomonas reinhardtii*. *J. Biotechnol.* **162**, 13–20.

Li, Y., Han, D., Hu, G., Dauvillee, D., Sommerfeld, M., Ball, S. and Hu, Q. (2010) *Chlamydomonas* starchless mutant defective in ADP-glucose pyrophosphorylase hyper-accumulates triacylglycerol. *Metab. Eng.* **12**, 387–391.

Merchant, S.S., Prochnik, S.E., Vallon, O., Harris, E.H., Karpowicz, S.J., Witman, G.B., Terry, A., Salamov, A., Fritz-Laylin, L.K., Marechal-Drouard, L., Marshall, W.F., Qu, L.H., Nelson, D.R., Sanderfoot, A.A., Spalding, M.H., Kapitonov, V.V., Ren, Q., Ferris, P., Lindquist, E., Shapiro, H., Lucas, S.M., Grimwood, J., Schmutz, J., Cardol, P., Cerutti, H., Chanfreau, G., Chen, C.L., Cognat, V., Croft, M.T., Dent, R., Dutcher, S., Fernandez, E., Fukuzawa, H., Gonzalez-Ballester, D., Gonzalez-Halphen, D., Hallmann, A., Hanikenne, M., Hippler, M., Inwood, W., Jabbari, K., Kalanon, M., Kuras, R., Lefebvre, P.A., Lemaire, S.D., Lobanov, A.V., Lohr, M., Manuell, A., Meier, I., Mets, L., Mittag, M., Mittelmeier, T., Moroney, J.V., Moseley, J., Napoli, C., Nedelcu, A.M., Niyogi, K., Novoselov, S.V., Paulsen, I.T., Pazour, G., Purton, S., Ral, J.P., Riano-Pachon, D.M., Riekhof, W., Rymarquis, L., Schroda, M., Stern, D., Umen, J., Willows, R., Wilson, N., Zimmer, S.L., Allmer, J., Balk, J., Bisova, K., Chen, C.J., Elias, M., Gendler, K., Hauser, C., Lamb, M.R., Ledford, H., Long, J.C., Minagawa, J., Page, M.D., Pan, J., Pootakham, W., Roje, S., Rose, A., Stahlberg, E., Terauchi, A.M., Yang, P., Ball, S., Bowler, C., Dieckmann, C.L., Gladyshev, V.N., Green, P., Jorgensen, R., Mayfield, S., Mueller-Roeber, B., Rajamani, S., Sayre, R.T., Brokstein, P., Dubchak, I., Goodstein, D., Hornick, L., Huang, Y.W., Jhaveri, J., Luo, Y., Martinez, D., Ngau, W.C., Otillar, B., Poliakov, A., Porter, A., Szajkowski, L., Werner, G., Zhou, K., Grigoriev, I.V., Rokhsar, D.S. and Grossman, A.R. (2007) The *Chlamydomonas* genome reveals the evolution of key animal and plant functions. *Science*, **318**, 245–250.

Merchant, S.S., Kropat, J., Liu, B., Shaw, J. and Warakanont, J. (2012) TAG, you're it! *Chlamydomonas* as a reference organism for understanding algal triacylglycerol accumulation. *Curr. Opin. Biotechnol.* **23**, 352–363.

Moellering, E.R. and Benning, C. (2010) RNA interference silencing of a major lipid droplet protein affects lipid droplet size in *Chlamydomonas reinhardtii*. *Eukaryot. Cell*, **9**, 97–106.

Montero, M., Aristizábal, M. and García Reina, G. (2011) Isolation of high-lipid content strains of the marine microalga *Tetraselmis suecica* for biodiesel production by flow cytometry and single-cell sorting. *J. Appl. Phycol.* **23**, 1053–1057.

Pinzon, N.M., Aukema, K.G., Gralnick, J.A. and Wackett, L.P. (2011) Nile red detection of bacterial hydrocarbons and ketones in a high-throughput format. *MBio*, **2**, e00109–e00111.

Radakovits, R., Jinkerson, R.E., Darzins, A. and Posewitz, M.C. (2010) Genetic engineering of algae for enhanced biofuel production. *Eukaryot. Cell*, **9**, 486–501.

Siaut, M., Cuine, S., Cagnon, C., Fessler, B., Nguyen, M., Carrier, P., Beyly, A., Beisson, F., Triantaphylides, C., Li-Beisson, Y. and Peltier, G. (2011) Oil accumulation in the model green alga *Chlamydomonas reinhardtii*: characterization, variability between common laboratory strains and relationship with starch reserves. *BMC Biotechnol.* **11**, 7.

Van den Koornhuyse, N., Libessart, N., Delrue, B., Zabawinski, C., Decq, A., Iglesias, A., Carton, A., Preiss, J. and Ball, S. (1996) Control of starch composition and structure through substrate supply in the monocellular alga *Chlamydomonas reinhardtii*. *J. Biol. Chem.* **271**, 16281–16287.

Wang, Z.T., Ullrich, N., Joo, S., Waffenschmidt, S. and Goodenough, U. (2009) Algal lipid bodies: stress induction, purification, and biochemical characterization in wild-type and starchless *Chlamydomonas reinhardtii*. *Eukaryot. Cell*, **8**, 1856–1868.

White, T., Bursten, S., Federighi, D., Lewis, R.A. and Nudelman, E. (1998) High-resolution separation and quantification of neutral lipid and phospholipid species in mammalian cells and sera by multi-one-dimensional thin-layer chromatography. *Anal. Biochem.* **258**, 109–117.

Work, V.H., Radakovits, R., Jinkerson, R.E., Meuser, J.E., Elliott, L.G., Vinyard, D.J., Laurens, L.M., Dismukes, G.C. and Posewitz, M.C. (2010) Increased lipid accumulation in the *Chlamydomonas reinhardtii* sta7-10 starchless isoamylase mutant and increased carbohydrate synthesis in complemented strains. *Eukaryot. Cell*, **9**, 1251–1261.

Zabawinski, C., Van Den Koornhuyse, N., D'Hulst, C., Schlichting, R., Giersch, C., Delrue, B., Lacroix, J.M., Preiss, J. and Ball, S. (2001) Starchless mutants of *Chlamydomonas reinhardtii* lack the small subunit of a heterotetrameric ADP-glucose pyrophosphorylase. *J. Bacteriol.* **183**, 1069–1077.

Supporting information

Additional Supporting information may be found in the online version of this article:

Figure S1 Nile Red bright colony phenotype.
Figure S2 TLC of representative lipid hyperaccumulating 21gr- (a) and 21st1-derived (b) mutants.
Figure S3 Visualization of Nile Red stained lipid bodies and flow cytometry analysis of Nile Red fluorescence staining intensities of 21gr-derived (a) and 21st1-derived (b) lipid hyperaccumulating mutants.
Table S1 Influence of culture phase and nitrogen-deprivation treatments on 21gr lipid yields.
Table S2 Lipid contents and yields, biomass yields and starch contents of low-starch strain 21st1.
Table S3 Identification of fatty acids from *C. reinhardtii* 21gr and 21st1by GC-MS.